

# 行政院國家科學委員會專題研究成果報告

## (Ln, A) (Mn, B) -O (Ln=La, Nd, Pr, Sm, ...) 材料的磁極傳輸特性系統化研究

計畫編號：NSC 89-2112-M-164-002-

執行期限：89 年 8 月 1 日至 90 年 7 月 31 日

主持人：陳宏仁副教授 修平技術學院電機工程系

### 一、中英文摘要

此研究使用標準陶磁技術製作  $\text{La}_{0.6}\text{Ln}_{0.1}\text{Pb}_{0.3}\text{MnO}_3$  (Ln=Pr, Nd and Y) 磁性材料塊材樣品。順磁-鐵磁轉變溫度會隨 La 位置部份取代而改變。Pr, Nd 及 Y 摻雜在低磁場的 FC-ZFC 曲線顯示似  $\lambda$ -形狀這表示材料具短程有旋序相。此因 Pr, Nd 及 Y 的離子半徑比 La 離子半徑小, 造成它們的鈣鈦礦結構產生大的扭曲。對 Pr 及 Nd 摻雜, 由於具 f-殼電子的 Pr 及 Nd 磁性離子的傾斜自旋, 在低磁場下磁矩難飽和, 而在高磁場下磁化率仍保持未飽和。

#### Abstract

$\text{La}_{0.6}\text{Ln}_{0.1}\text{Pb}_{0.3}\text{MnO}_3$  (Ln=Pr, Nd and Y) oxides have been synthesized by standard Ceramic method. The paramagnetic-ferromagnetic transition temperature values alter considerably by partially substituting different rare earth ions at the La site. The low field FC-ZFC curves of Pr-doped, Nd-doped and Y-doped manganites display a  $\lambda$ -shape-like behavior hinting for a short-range spin order phase. These facts are in good agreement with the smaller ionic radii of Pr, Nd and Y ions, which are contrary to La ionic radius, and with the corresponding large distortion of their perovskite structures. For Pr-doped and Nd-doped manganites, due to the canted spin of magnetic Pr and Nd ions with f-shell electrons, the magnetic moments

are hardly saturated in low field and the magnetization remains unsaturated in high field.

### 二、緣由與目的

Perovskite manganese oxides,  $\text{Ln}_{1-x}\text{A}_x\text{MnO}_3$  (Ln = La, Nd, Pr, Sm etc., and A = Ca, Sr, Ba, Pb etc.), have recently attracted considerable attention because of rich variety of crystallographic, magnetic and electronic phases<sup>1-2</sup>.  $\text{LaMnO}_3$ , the prototype of these perovskite oxides, is an antiferromagnetic insulator with an orthorhombic distortion structure<sup>3</sup>. The partial substitution of divalent ions for the trivalent rare earth ions induces ferromagnetism in these compounds due to the conversion of  $\text{Mn}^{+3} (t_{2g}^3 e_g^1)$  into  $\text{Mn}^{+4} (t_{2g}^3 e_g^0)$ . Historically the theory of double exchange (DE) has been led to explain this phenomenon and successfully explained  $x = 0.3$  is the optimally doped composition<sup>4-5</sup>. Recent works have shown that the mechanism of magnetic polarons formed by the Jahn-Teller distortion of the  $\text{MnO}_6$  octahedral may be responsible for explaining the CMR effect with the DE model<sup>6-7</sup>. The introduction of smaller Ln-site ions can lead to a larger deformation of the octahedral in the perovskites, bend the Mn-O-Mn bonds and, consequently, weaken the DE interaction

between  $Mn^{+3}$  and  $Mn^{+4}$ . It is appealing that there seems a direct relation between the complex lattice effects and the tolerance factor,  $t = (r_{Ln} + r_O) / \sqrt{2}(r_{Mn} + r_O)$ , a geometrical parameter describing the inhomogeneity in the  $LnMnO_3$  perovskite compounds<sup>8</sup>. The substitution of La by smaller ion is expected to enhance the microstructure inhomogeneity that may play an important role in the properties of the spin-lattice coupling and magnetic behaviors.

### 三、結果與討論

Polycrystalline bulk samples of the compounds  $La_{0.6}Ln_{0.1}Pb_{0.3}MnO_3$  ( $Ln = Pr, Nd$  and  $Y$ ) were prepared by conventional ceramic fabrication technique of solid-state reaction. The start reagents,  $La_2O_3$ ,  $Pr_6O_{11}$ ,  $Nd_2O_3$ ,  $YO_3$ ,  $PbCO_3$  and  $MnCO_3$ , were mixed with a stoichiometric proportions. The powders were calcined twice in air at 850 for 24 hours with intermediate grindings, then pressed into disk-shaped pellets and finally sintered in air at 1175 for 72 hours. The structure and phase purity of the samples were examined by the powder  $x$ -ray diffraction using  $Cu-K\alpha$  radiation at room temperature. The magnetization measurements were performed by a Quantum Design MPMS superconducting quantum interference device (SQUID) magnetometer.

For comparative purpose, the  $x$ -ray powder diffraction diagram of four respective samples,  $La_{0.7}Pb_{0.3}MnO_3$  (LP),  $La_{0.6}Pr_{0.1}Pb_{0.3}MnO_3$  (LPP),  $La_{0.6}Nd_{0.1}Pb_{0.3}MnO_3$  (LNP) and  $La_{0.6}Y_{0.1}Pb_{0.3}MnO_3$  (LYP), are shown in Fig.1. The powder  $x$ -ray diffraction patterns show single-phase rhombohedral crystal

structure with space group  $R\bar{3}c$  (No. 167) for the former three compositions, while the last composition had orthorhombic symmetry with space group  $Pnma$  (No. 62). The ionic radii of cations  $La^{3+}$ ,  $Pr^{3+}$ ,  $Nd^{3+}$  and  $Y^{3+}$  are 0.136, 0.129, 0.127 and 0.119 nm, respectively<sup>9</sup>. In this series of samples, the peaks of  $x$ -ray patterns gradually shift to higher degree due to the partial substitution of smaller ion,  $Pr^{3+}$ ,  $Nd^{3+}$  and  $Y^{3+}$ , in the La-site. Tolerance factors of the partially substituted phases of smaller ion are lower than those obtained for the La compound. As  $t$  decreases in the perovskite structure, the Mn-O bond compressed and the A-O bond becomes tense<sup>10</sup>. Consequently, substituting smaller ion for La bends the Mn-O-Mn bond angle to  $(180^\circ - \zeta)$  and  $\zeta$  increases when  $t$  decreases. However, the  $t$  values, listed in Table I, are greater than 0.9853 in all cases, hinting good stability of the structure.

In order to get more insight into the spin order and magnetic behavior, we measured the ZFC (zero-field-cool) and FC (field-cool) magnetization-temperature (M-T) curves in the field of 100 Oe. The method of low field ZFC-FC measurement is one of the methods generally used to characterize short-range spin order behavior. The ZFC-FC curves of all samples are presented in Fig. 2. The saturation moment of Mn spins in LP compound clearly suggests a ferromagnetic long-range spin order. Conversely, the ZFC-FC curves display the irreversibility and  $\omega$ -shape traces with LPP, LNP and LYP compositions, suggesting the nature of a short-range spin order. The ZFC curves coincide with the FC curves at high temperature, but become apparently decreasing as  $t$

decreased below ferromagnetic-paramagnetic transition temperature  $T_c$  which is defined as the temperature where the  $dM/dT$  reaches the minimum value. Analogous magnetic behaviors are also reported when  $\text{La}^{+3}$  is partially substituted by other trivalent rare earth ions<sup>11</sup>.  $T_c$  values, listed in Table I, alter considerably due to the decrease of  $t$  values, the effect of lattice distortion and Mn-O-Mn bonds bending induced by substituting smaller rare earth ions for La.

The Magnetic hysteresis loops at 5K with -5T to 5T applied field are shown in Fig. 3. The magnetization of LPP, LNP and LYP increase slowly than that of LP due to the smaller  $t$  values in low magnetic field. It is reasonable to conclude that the observed behavior corresponds to the spin order in which short-range spin order is harder to be magnetized than the long-range one. The magnetization are easily saturated by external magnetic field with the LP and LYP compounds which show essentially no high-field slope, listed in Table II, indicative of a collinear ferromagnetic state. LPP and LNP remain unsaturated in the high fields, showing the slopes of  $0.0797 \sim_B/T$  with LPP and  $0.1981 \sim_B/T$  with LNP. The manganese sublattice is ferromagnetic while the magnetic ions  $\text{Pr}^{+3}$  and  $\text{Nd}^{+3}$  with  $f$ -shell electrons seem gradually aligned with the manganese as field increases. Thus, the latter contributes to an additional value to the total moment for LPP and LNP samples. The saturation moments,  $M_s$ , extrapolated to zero field from hysteresis curves are listed in Table II. The results are consistent with the data of high-field slope.

#### 四、計劃成果及自評

We have presented a systematical study of the magnetotransport behavior in the  $(\text{La}_{0.6}\text{Ln}_{0.1})\text{Pb}_{0.3}\text{MnO}_3$  system. Regarding their structures and magnetic properties, the LP compound is different from LPP, LNP and LYP compounds. The ZFC-FC magnetization results have shown that the substitution of Pr, Nd and Y for La in  $\text{La}_{0.7}\text{Pb}_{0.3}\text{MnO}_3$  induces the structural distortion and leads the oxide to a short-range spin order state. The magnetization is easily saturated by external magnetic field for the LP and LYP compounds with essentially no high-field slope. Conversely, the magnetization of LPP and LNP remain unsaturated in the high fields. We may, therefore, conclude that the observed behavior corresponds to : (i) the structure tuning induced by the small ionic radius of the interpolated cation in the Ln site, (ii) the magnetic ionic characteristic of  $\text{Nd}^{+3}$  and  $\text{Pr}^{+3}$ , which is in contrary to the nonmagnetic  $\text{La}^{+3}$  and  $\text{Y}^{+3}$  ion.

#### 五、參考文獻

1. K. Ghosh, S. B. Ogale, R. Ramesh, R. L. Greene, T. Venkatesan, R. S. Bathe, S. I. Patil, Phys. Rev. B **59**, 533 (1999).
2. J. B. Goodenough, J. Appl. Phys. **81**, 5330 (1997).
3. C. N. R. Rao, R. Mahesh, and R. M. ahendiran, J. Phys. Chem. Solids, **59**, 487 (1998).
4. C. Zener, Phys. Rev. **82**, 403 (1951).
5. P. Schiffer, A. P. Ramirez, W. Bao, and S. W. Cheong, Phys. Rev. Lett. **75**, 3336 (1995).
6. L. Sheng, D. Y. Xing, D. N. Sheng, and C. S. Ting, Phys. Rev. Lett. **79**, 1710 (1997).
7. P. S. Anil Kumar, P. A. Joy and S. K. Date,

- J. Phys.: Condens. Matter, **10**, L269(1998).
8. H. Y. Wang, S. -W Choeng, R. G. Radaelli, M. Marezio, and B. Batlogg, Phys. Rev. Lett. **75**, 914 (1995).
9. R.D. Shannon and C.T. Prewitt, Acta Crystallogr. Sec. A **32**, 751 (1976)10. S. N. Okuno and K. Inomata, Phys. Rev. Lett. **72**, 1553 (1994).
10. J. B. Goodenough, J. Appl. Phys. **81**, 5330 (1997).
11. J. M. De Teresa, M. R. Ibarra, J. Garcia, J. Blasco, C. Ritter, P. A. Algarable, C. Marquina, and A. del Moral, Phys. Rev. Lett. **76**, 1727 (1996).]

Table I. The tolerance factor  $t$ , phase symmetry and transition temperature  $T_c$  for all samples.

Composition	$t$	phase <sup>a</sup>	$T_c$ (K)
$\text{La}_{0.7}\text{Pb}_{0.3}\text{MnO}_3$	0.9915	R	332
$(\text{La}_{0.6}\text{Pr}_{0.1})\text{Pb}_{0.3}\text{MnO}_3$	0.9889	R	316
$(\text{La}_{0.6}\text{Nd}_{0.1})\text{Pb}_{0.3}\text{MnO}_3$	0.9883	R	386
$(\text{La}_{0.6}\text{Y}_{0.1})\text{Pb}_{0.3}\text{MnO}_3$	0.9853	O	238

<sup>a</sup>R-rhombohedral, O-orthorhombic

Table II. The saturation moment  $M_s$  (extrapolated to 0 T) and high-field slope for all sample.

Composition	$M_s$ (emu/g)	High-field slope ( $\mu_B/T$ )
$\text{La}_{0.7}\text{Pb}_{0.3}\text{MnO}_3$	78.86	0.0012
$(\text{La}_{0.6}\text{Pr}_{0.1})\text{Pb}_{0.3}\text{MnO}_3$	81.08	0.0266
$(\text{La}_{0.6}\text{Nd}_{0.1})\text{Pb}_{0.3}\text{MnO}_3$	84.83	0.0701
$(\text{La}_{0.6}\text{Y}_{0.1})\text{Pb}_{0.3}\text{MnO}_3$	76.81	0.0015

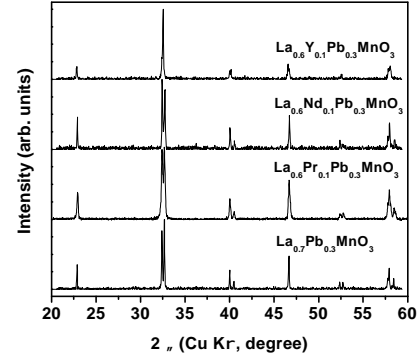


Fig. 1. X-ray patterns of three samples for all samples.

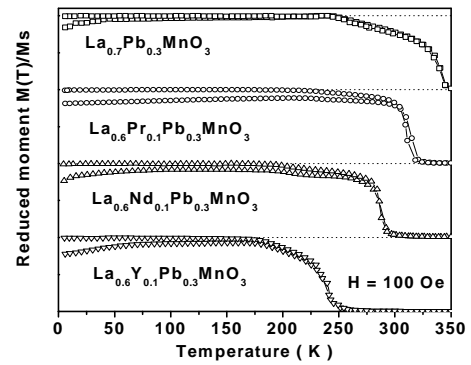


Fig. 2. Temperature dependence of magnetization at a low field of 100Oe for all samples..

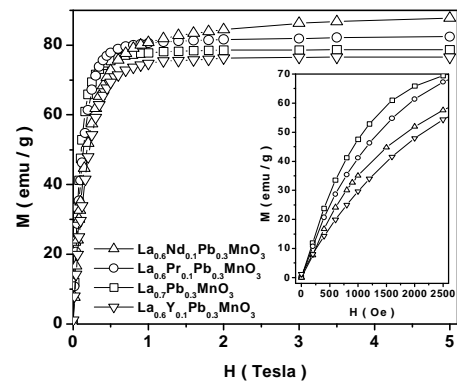


Fig. 3. Magnetic hysteresis loops at 5K with -5T to 5T applied field for all samples.